Four amino acids define the CO_2 binding pocket of enoyl-CoA carboxylases/reductases

Gabriele M. M. Stoffel[a,b], David Adrian Saez[c], Hasan DeMirci[d,e], Bastian Vögeli[a], Yashas Rao[d], Jan Zarzycki[a,b], Yasuo Yoshikuni[f], Soichi Wakatsuki[d,g,1], Esteban Vöhringer-Martinez[c,1], and Tobias J. Erb[a,b,1]

[a]Department of Biochemistry and Synthetic Metabolism, Max Planck Institute for Terrestrial Microbiology, D-35043 Marburg, Germany; [b]Center for Synthetic Microbiology, D-35043 Marburg, Germany; [c]Departamento de Físico Química, Facultad de Ciencias Químicas, Universidad de Concepción, 4070371 Concepción, Chile; [d]Biosciences Division, SLAC National Accelerator Laboratory, Menlo Park, CA 94025; [e]Stanford PULSE Institute, SLAC National Accelerator Laboratory, Menlo Park, CA 94025; [f]Department of Energy Joint Genome Institute, Walnut Creek, CA 94598; and [g]Structural Biology Department, Stanford University, Stanford, CA 94305

Edited by James C. Liao, Institute of Biological Chemistry, Academia Sinica, Taipei, Taiwan, and approved June 3, 2019 (received for review January 30, 2019)

Carboxylases are biocatalysts that capture and convert carbon dioxide (CO_2) under mild conditions and atmospheric concentrations at a scale of more than 400 Gt annually. However, how these enzymes bind and control the gaseous CO_2 molecule during catalysis is only poorly understood. One of the most efficient classes of carboxylating enzymes are enoyl-CoA carboxylases/reductases (Ecrs), which outcompete the plant enzyme RuBisCO in catalytic efficiency and fidelity by more than an order of magnitude. Here we investigated the interactions of CO_2 within the active site of Ecr from *Kitasatospora setae*. Combining experimental biochemistry, protein crystallography, and advanced computer simulations we show that 4 amino acids, N81, F170, E171, and H365, are required to create a highly efficient CO_2-fixing enzyme. Together, these 4 residues anchor and position the CO_2 molecule for the attack by a reactive enolate created during the catalytic cycle. Notably, a highly ordered water molecule plays an important role in an active site that is otherwise carefully shielded from water, which is detrimental to CO_2 fixation. Altogether, our study reveals unprecedented molecular details of selective CO_2 binding and C–C-bond formation during the catalytic cycle of nature's most efficient CO_2-fixing enzyme. This knowledge provides the basis for the future development of catalytic frameworks for the capture and conversion of CO_2 in biology and chemistry.

carboxylases | enzyme mechanisms | carbon dioxide | CO_2 fixation | RuBisCO

The efficient capture and conversion of atmospheric carbon dioxide (CO_2) is a prerequisite to develop a carbon-neutral, circular future economy. In biology, carbon fixation is performed under mild conditions and at atmospheric concentrations of CO_2 (0.04 vol.%) by enzymes called carboxylases (1). It is estimated that 400 Gt of CO_2 are fixed annually by a single biocatalyst, ribulose-1,5-bisphophate-carboxylase/oxygenase (RuBisCO), the key enzyme of photosynthesis (2, 3). In comparison, the chemical conversion of CO_2 in industry accounts for only 0.1 Gt of carbon annually and uses pressurized CO_2 (4), which emphasizes our need to understand the molecular mechanism that allows (bio) catalysts to selectively interact with a low-concentrated CO_2 molecule during catalysis.

Carboxylases catalyze the formation of a C–C bond between an acceptor substrate and a CO_2 molecule (1) where the latter represents the electrophile (5). To facilitate C–C bond formation, most carboxylases activate their respective nucleophilic substrate (usually a thioester, α-ketoacid, or ketone) by converting it into an enol(ate) (6). Enol(ate)s are strong nucleophiles and highly reactive. A key requirement of CO_2-fixation catalysis is the tight control of the reaction between the activated acceptor substrate and CO_2. Any loss of catalytic control over the enol(ate) or the CO_2 molecule bears the danger of side reactions and reduces the efficiency of carbon fixation (7). The most prominent example is RuBisCO, which is known to feature several side reactions, most notably an oxygenation reaction (8). One in every 5 turnovers RuBisCO will incorporate an oxygen (O_2) molecule instead of CO_2, which leads to the formation of 2-phosphoglycolate, a side product that is toxic to the cell and has to be recycled in an energy-demanding process, highlighting the need of carboxylases to control the reaction of the activated acceptor with CO_2.

Another challenge in this respect is the accessibility of water (or protic amino acids) to the active site of carboxylases. Protons are better electrophiles than the CO_2 molecule, which can directly quench the enolate. As a consequence, it is not sufficient that carboxylases enrich a low abundant gaseous CO_2 molecule; they also need to efficiently suppress any competing (re)protonation reactions. Altogether, these examples show that controlling the fate of CO_2 at the molecular level is a crucial feature of carboxylases. However, to date only very limited biochemical, let alone structural, information on CO_2 binding in carboxylases (and other proteins) is available, besides some theoretical considerations (9–14).

Here, we focused on a class of carboxylases, enoyl-CoA carboxylases/reductases (Ecrs) (15, 16) that show the fastest turnover frequencies among all carboxylases to date and exclusively

Significance

Carboxylases capture and convert CO_2, which makes them key enzymes in photosynthesis and the global carbon cycle. However, the question how enzymes bind atmospheric CO_2 is still unsolved. We studied enoyl-CoA carboxylases/reductases (Ecrs), the fastest CO_2-fixing enzymes in nature, using structural biology, biochemistry, and advanced computational methods. Ecrs create a highly specific CO_2-binding pocket with 4 amino acids at the active site. The pocket controls the fate of the gaseous molecule during catalysis and shields the catalytic center from oxygen and water. This exquisite control makes Ecrs highly efficient carboxylases outcompeting RuBisCO, the key enzyme of photosynthesis, by an order of magnitude. Our findings define the atomic framework for the future development of CO_2-converting catalysts in biology and chemistry.

Author contributions: G.M.M.S., D.A.S., H.D., B.V., Y.R., S.W., E.V.-M., and T.J.E. designed research; G.M.M.S., D.A.S., H.D., Y.R., and E.V.-M. performed research; D.A.S. and Y.Y. contributed new reagents/analytic tools; G.M.M.S., D.A.S., H.D., Y.R., and J.Z. analyzed data; and G.M.M.S., D.A.S., H.D., Y.R., S.W., E.V.-M., and T.J.E. wrote the paper.

The authors declare no conflict of interest.

This article is a PNAS Direct Submission.

Data deposition: Crystallography, atomic coordinates, and structure factors have been deposited in the Protein Data Bank (PDB), http://www.rcsb.org/; PDB ID code: 6OWE.

[1]To whom correspondence may be addressed. Email: toerb@mpi-marburg.mpg.de, soichi.wakatsuki@stanford.edu (for X-ray crystallography), or evohringer@udec.cl (for computational correspondence).

This article contains supporting information online at www.pnas.org/lookup/suppl/doi:10.1073/pnas.1901471116/-/DCSupplemental.

Published online June 26, 2019.

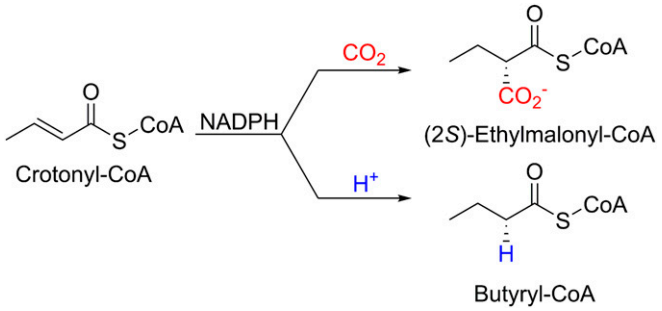

Scheme 1. Reaction catalyzed by Ccr. Carboxylation to (2*S*)-ethylmalonyl-CoA in the presence of CO_2 and reduction to butyryl-CoA in the absence of CO_2.

react with CO_2 in the presence of O_2. These features make Ecrs excellent model systems to understand the details of selective CO_2 binding and C–C-bond formation in proteins.

The best-studied Ecr is crotonyl-CoA carboxylase/reductase (Ccr) that catalyzes the NADPH-dependent reductive carboxylation of crotonyl-CoA into (2*S*)-ethylmalonyl-CoA. While Ccr does not show side reactivity with O_2, the enzyme catalyzes the reduction of crotonyl-CoA to butyryl-CoA as a side reaction, but only in the absence of CO_2 and at low catalytic efficiency (Scheme 1) (17, 18). It has been suggested that this side reaction is an evolutionary remnant of Ecrs, which are evolutionary related to enoyl thioester reductases that catalyze the ordinary reduction of enoyl-CoA esters (6, 19). Apparently, Ecrs evolved from simple reductases into reductive carboxylases by acquiring a CO_2-fixation function along their evolutionary trajectory.

In a previous structural study, CinF, an Ecr from *Streptomyces sp. JS360*, was crystallized with $NADP^+$ and octenoyl-CoA [Protein Data Bank (PDB); PDB ID code: 4A0S (20)]. A putative CO_2 binding pocket was proposed to be composed of Asn77, Phe166, and Glu167, which are all highly conserved in Ecrs. It was suggested that CO_2 is held in position by hydrogen bonding to Asn77 and Glu167 while Phe166 would undergo hydrophobic interactions with CO_2. Mutation of these residues suppressed the carboxylation of octenoyl-CoA (20). However, the exact role of the individual residues directing and controlling the carboxylation reaction remains enigmatic: in particular, how the gaseous CO_2 molecule is aligned at the active site and how the reduction side reaction is efficiently suppressed.

Here we combine experimental biochemistry, protein crystallography, and computer simulations to define the molecular interactions of CO_2 during C–C-bond formation at the active site of Ecrs. Our results suggest that 4 amino acids are sufficient to convert an ordinary reductase into a highly efficient carboxylase. Together, these 4 residues anchor and lock the CO_2 molecule in a favorable position for the attack by the reactive enolate created during catalysis. Notably, a highly ordered water molecule plays an essential role in coordinating the CO_2 molecule, while the active site is otherwise effectively shielded from water to suppress the reduction side reaction. Altogether our computational and experimental studies reveal the details of selective CO_2 binding and C–C-bond formation in the catalytic cycle of nature's most efficient CO_2-fixing enzyme.

Results

Crystal Structure of KsCcr with Ethylmalonyl-CoA and NADPH. We solved the structure of Ccr from *Kitasatospora setae* (KsCcr) cocrystallized with NADPH and soaked with ethylmalonyl-CoA, the product of the carboxylation reaction, at 1.7-Å resolution (Fig. 1 and *SI Appendix*, Table S1, PDB ID code: 6OWE). The active site of KsCcr shares similar features with the CinF homolog previously reported (20) [PDB ID codes: 4A0S (20), 4Y0K (21), and 4GI2]. In contrast to these structures that did not capture the interaction of the protein with CO_2, neither as free gas or covalently bound to the acyl-CoA moiety, our structure shows densities that can be interpreted as carboxylated product (*SI Appendix*, Fig. S1). This enabled us to identify 4 residues that potentially interact with CO_2, namely Asn81, Phe170, Glu171, and His365. His365 also interacts with NADPH via hydrogen bonding (3.0 Å) to the carboxamide group of the nicotinamide, indicating a second function of His365 in coordinating the NADPH cofactor during catalysis. Similar to previously published structures we also observed an ordered water molecule between His365 and Glu171 at a distance of 2.9 and 2.7 Å, respectively. This feature is absent in structures lacking substrate and cofactor (PDB ID codes: 3HZZ and 3KRT) suggesting a role of the water molecule in the active enzyme complex. To test the function of these residues during catalysis, we characterized different active site variants and addressed the reaction mechanism with molecular-dynamics simulations along the

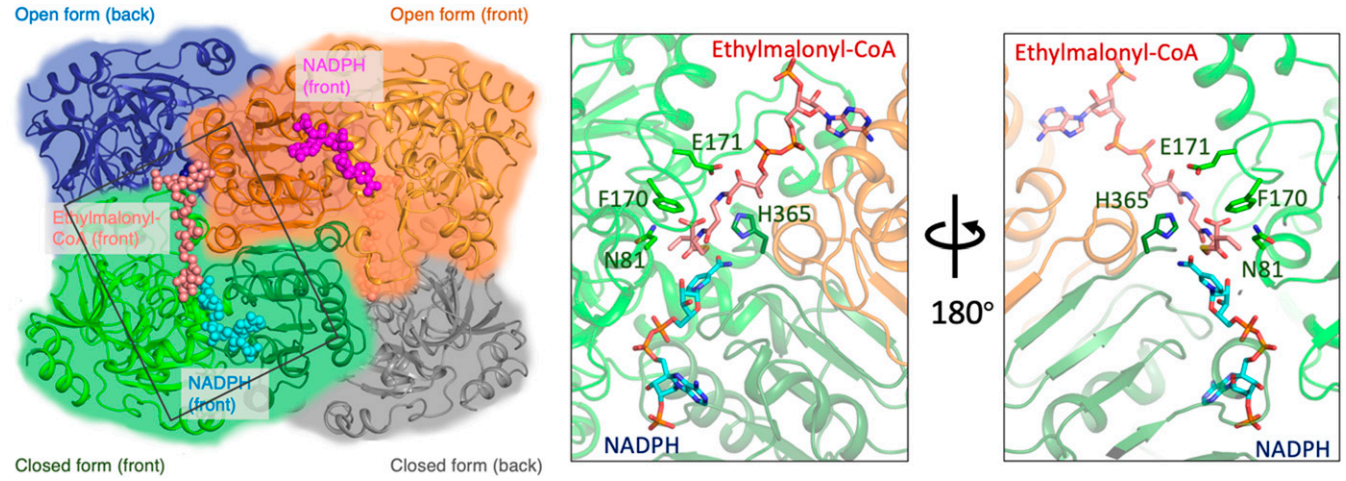

Fig. 1. Structure of KsCcr complexed with NADPH and ethylmalonyl-CoA. (*Left*) KsCcr forms a dimer of dimers of open- and closed-form subunits. The subunits are highlighted in gray and green (closed form with NADPH and ethylmalonyl-CoA, both represented in spheres) and blue and orange (open form with NADPH only, represented in spheres). The rectangle represents close-up of the active site shown in the middle and right. (*Middle*) The active site with the CO_2-binding residues His365, Glu171, Phe170, and Asn81 in green, ethylmalonyl-CoA (salmon), and NADPH (cyan); oxygen and nitrogen atoms are colored in red and blue, respectively. (*Right*) Same as *Middle* but rotated by 180° about the viewing direction.

minimum free-energy path within the quantum mechanics/molecular mechanics methodology.

Kinetic Characterization of KsCcr Wild Type. KsCcr wild type (WT) showed an apparent turnover frequency (k_{cat}) of 103 ± 3 s^{-1} which is well in line with previously reported value of 104 s^{-1} for the Ccr of *Rhodobacter Sphaeroides* (16). Apparent K_M values were 21 ± 2 μM (crotonyl-CoA), 37 ± 4 μM (NADPH), and 90 ± 10 μM (CO_2), respectively, and substrate inhibition for crotonyl-CoA was observed at a K_i of 3,650 ± 810 μM. Under saturating amounts of CO_2, the enzyme showed 100% carboxylation activity and exclusively formed (2*S*)-ethylmalonyl-CoA. In the absence of CO_2, the enzyme catalyzed the reduction of crotonyl-CoA to butyryl-CoA (Table 1). Stereochemical analysis of the butyryl-CoA in D_2O showed that 94 ± 2% of the deuterium label was retained (Table 1), demonstrating that the reduction side reaction took place in a stereospecific manner.

Asn81 Anchors the CO_2 Molecule. How is the CO_2 molecule bound in the active site? A key residue is Asn81, which defines one end of the putative CO_2 binding pocket. Simulations of the WT enzyme exhibited a hydrogen-bond interaction between the carboxamide NH_2 group of Asn81 and the CO_2 molecule (Fig. 2*A* and Movie S1). When we experimentally characterized the reaction of the N81L variant in more detail, we observed a strongly decreased carboxylation reaction, as well as accumulation of a covalent reaction intermediate, a so-called C2-ene adduct (*SI Appendix*, Fig. S3). C2-ene adducts are also observed in WT Ecrs when the catalytic cycle is stalled, for example when CO_2 is omitted from the reaction mixture. The fact that a C2-ene adduct is observed in the reaction of the N81L variant even under saturating CO_2 conditions suggests that the interaction of the enzyme with CO_2 is severely disturbed by the N81L mutation. Simulations of the N81L variant revealed that most of the catalytic residues and water molecules remain in the same position, while the CO_2 molecule appears increasingly disordered (Fig. 2*D* and Movie S2). As a consequence, the minimum energy profile from the C2-adduct to the product (2*S*)-ethylmalonyl-CoA of N81L becomes endothermic and shows significantly higher barriers for the C–C-bond formation step compared with the WT. This explains the reduced carboxylation activity, as well as the accumulation of the C2-ene adduct that we experimentally observed in the N81L variant (Fig. 2 *C* and *F*).

Our simulations show that the active site of N81L does not become more solvent accessible, so that the reduction side reaction is still suppressed at the enzyme's active site. But, why does N81L show 89% butyryl-CoA formation? Note that C2-ene adducts are unstable and prone to spontaneous decay into butyryl-CoA and $NADP^+$ in free solution. Accordingly, the "apparent" side reaction in N81L is nonenzymatic and caused by release of the C2-ene adduct from the active site followed by its spontaneous decay in the solvent, as described before (18, 22, 23). This hypothesis is supported by our observation that stereospecificity of butyryl-CoA formation is almost completely lost in N81L compared with the WT (Table 1). Altogether, our experimental findings are well in line with the higher calculated free-energy barriers for the carboxylation step and endothermic product formation in the N81L variant (Fig. 2*F*), highlighting how crucial Asn81 is for correct positioning of CO_2.

How is the interaction of the carboxamide group of Asn81 with CO_2 controlled? Analysis of the interaction network of the amino acid shows hydrogen bonding of Asn81 to 2 residues in the second shell of the active site, Thr82 and Ser119. We hypothesized that these interactions are essential in pointing the carboxamide NH_2 group Asn81 toward the active site to enforce its interaction with the CO_2 molecule. Indeed, the variants T82D and S119A showed almost full carboxylation, but at more than 50-fold reduced turnover frequency (*SI Appendix*, Table S3), demonstrating the importance of these secondary shell residues in increasing catalytic activity of Asn81. In summary, both simulation and experimental data suggest that Asn81 is crucial to position CO_2 and to establish favorable interactions of the gas molecule with the enzyme during catalysis. Absence of this residue leads to lowered carboxylation efficiency and increased formation of the labile C2-ene adduct, which is not further processed by the enzyme and leaves the active site upon which it spontaneously decays in solution.

Phe170 Shields the Active Site from Water. The reactive nature of the enolate that is formed during the catalytic cycle of Ccr mandates that the enolate does not get into contact with water at the active site, which would inevitably lead to its protonation and

Table 1. Apparent steady-state parameters for KsCcr and its mutants expressed as mean value ± SE

Enzyme	Substrate	K_M, μM	K_i, μM	k_{cat}, s^{-1}	% EMC*	% Label retention†
WT	Crotonyl-CoA	21 ± 2	3,650 ± 810	103 ± 3	100	94.3 ± 1.8
	NADPH	37 ± 4	—	86 ± 2		
	CO_2‡	90 ± 10	—	78 ± 2		
N81L	Crotonyl-CoA	ND§	ND	ND	19	58.9 ± 1.1
	NADPH	ND	ND	ND		
F170Y	Crotonyl-CoA	10 ± 1	558 ± 80	83 ± 4	100	ND
	NADPH	36 ± 3	—	56 ± 1		
	CO_2‡	150 ± 20	—	56 ± 2		
F170A	Crotonyl-CoA	31 ± 6	—	8.3 ± 0.4	17	87 ± 0.6
	NADPH	11 ± 0.6	—	11 ± 0.1		
H365N	Crotonyl-CoA	29.8 ± 4.2	—	5.0 ± 0.2	93	63.3 ± 0.5
	NADPH	22 ± 2	—	8.1 ± 0.3		
	CO_2‡	1310 ± 220	—	7.4 ± 0.7		
E171A	Crotonyl-CoA	500 ± 62	—	5.1 ± 0.2	97	91.4 ± 0.2
	NADPH	112 ± 8	—	6.0 ± 0.2		
	CO_2	155 ± 30	—	5.1 ± 0.3		

SI Appendix, Fig. S2 shows the Michaelis–Menten graphs of the original data.
*Percentage of (2*S*)-ethylmalonyl-CoA (EMC) over total amount of products.
†Deuterium label retention at the α-position of crotonyl-CoA expressed as mean value ± SD.
‡Apparent K_M values for CO_2 were calculated from the HCO_3^- concentration in solution at pH = 8.
§Not determined due to accumulation of the covalent C2-ene adduct.

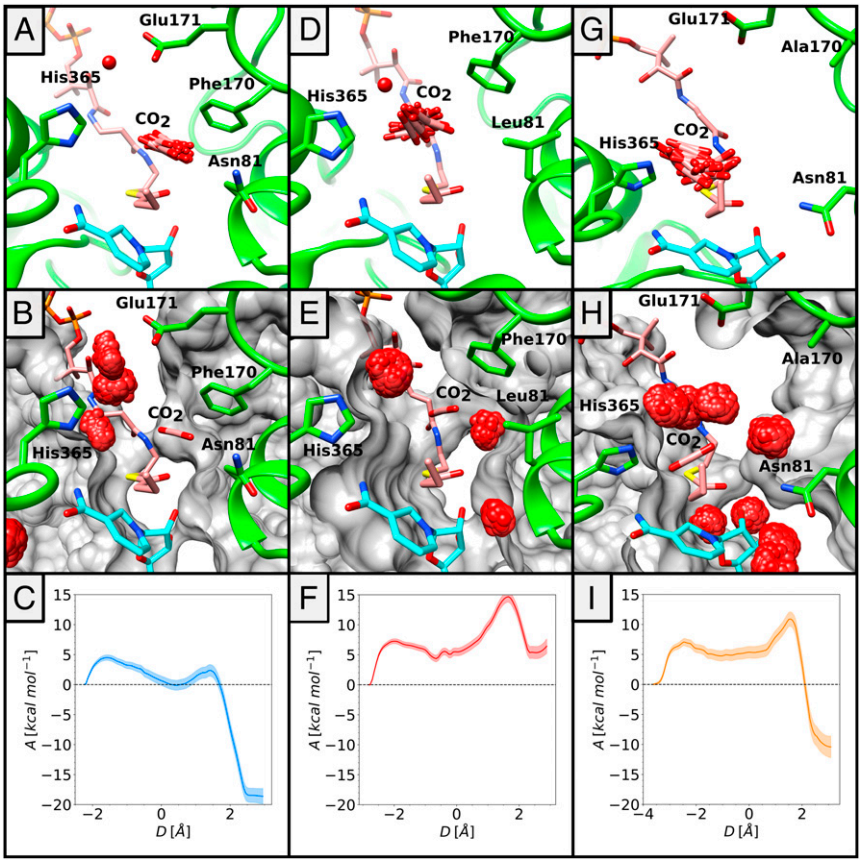

Fig. 2. *Left*, *Middle*, and *Right* columns represent the WT, N81L, and F170A variants respectively. (*A*, *D*, and *G*) Active site of KsCcr variants before the nucleophilic attack of the enolate onto CO_2. An overlay of different conformations of the CO_2 molecule visualizes the tumbling motion in the different enzyme variants. CoA-ester is shown in salmon and $NADP^+$ in cyan, and the red sphere represents the conserved water molecule coordinated by His365 and Glu171. (*B*, *E*, and *H*) Hydration sites located within 5 Å of the C_α obtained with SSTMap. For each enzyme, representative structures of the reactant state were subjected to 1 ns of constrained quantum mechanics/molecular mechanics simulations. The different positions sampled by the water molecules allowed the determination of clusters showing the preferential location of the solvent within the active site. (*C*, *F*, and *I*) Minimum free-energy path from the C2-ene adduct through the enolate to the products (2*S*)-ethylmalonyl-CoA and $NADP^+$. Parameter *D* represents the distance between C_α and C_2 minus the distance between C_α and CO_2.

formation of the butyryl-CoA side product. A role in shielding the active site from water had been previously suggested for Phe170 (20). Simulations of an F170A variant reveal conformational changes that result in a disorganization of the active site and an increase in the number of hydration sites compared with the WT (Fig. 2; compare Fig. 2 *B* and *H*, Movie S3, and *SI Appendix*, Supplementary Pymol and Chimera Files 1a and b and 3a and b). These changes also perturb the interaction of the CO_2 molecule with Asn81 (Fig. 2*G*). Accordingly, the CO_2 molecule loses its favorable position for the reaction with the enolate so that both activation barriers are increased (Fig. 2*I*), which is in agreement with our experimental data (Table 1). In the F170A variant the carboxylation activity is decreased to 17% at the expense of increased reduction side reactivity. Unlike in the N81L variant, however, protonation takes place in F170A with almost WT stereospecificity (Table 1), confirming that in the F170A enzyme water is able to reach the active site and directly protonate the enolate.

Some Ecrs feature a tyrosine at position 170 instead of the phenylalanine. When we tested an F170Y variant, the enzyme showed a slightly increased substrate inhibition, but otherwise very similar kinetic parameters as the WT. Most importantly, the F170Y variant displayed full conversion of crotonyl-CoA to (2*S*)-ethylmalonyl-CoA in the presence of saturating amounts of CO_2, indicating that the presence of the hydroxyl group does not affect carboxylation activity. In summary, these experiments together with the simulations showed that the phenyl rings of phenylalanine (and tyrosine) play an important role in suppressing the reduction reaction of Ecrs by water shielding.

His365 and Glu171 Coordinate an Ordered Water Molecule Interacting with CO_2. Opposite of Asn81 and at the other end of the putative CO_2-binding pocket the residues His365 and Glu171 are located. Together, these 2 residues coordinate a water molecule. In our simulations the ordered water molecule participates in hydrogen-bonded network of 3 water molecules, which interact directly with the CO_2 molecule during the carboxylation step (Fig. 3). What is the exact contribution of these 2 residues to catalysis, in particular in respect to CO_2 binding and water accessibility?

His365 serves a dual role by also coordinating the nicotinamide ring of NADPH. To preserve interaction of residue 365 with the NADPH cofactor, but interrupt its coordination of the ordered water molecule, we generated KsCcr H365N. The H365N variant showed a 20-fold decreased activity compared with the WT enzyme but still displayed 93% of carboxylated product, even though the K_M for CO_2 was raised by more than 1 order of magnitude. These data suggest that a defect in water coordination negatively affects C–C-bond formation activity in the H365N variant. However, this does not lead to a complete hydration of the active site. Simulations of the H365N mutant revealed broken interactions of the CO_2 molecule with Asn81 (Fig. 3*D* and Movie S4). The coordination to the ordered water molecule that bridges to Glu171 is lost, and the latter residue is rotated out of the active site disfavoring CO_2

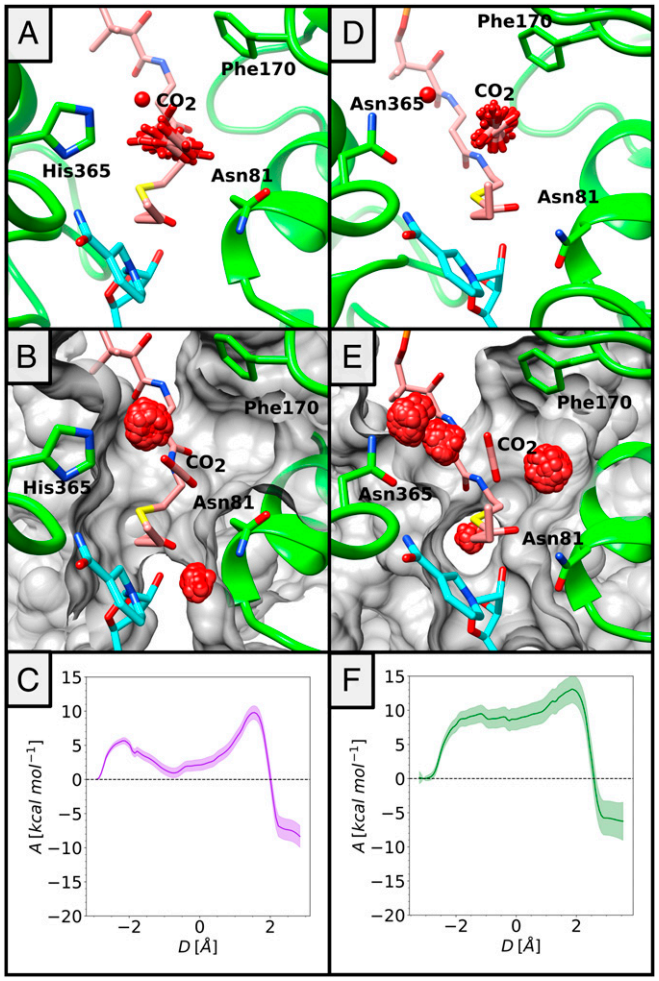

Fig. 3. *Left* and *Right* columns represent the E171A and H365 N variants, respectively. (*A* and *D*). Active site of KsCcr variants before the nucleophilic attack of the enolate onto CO_2. The CoA-ester is shown in salmon and $NADP^+$ in cyan. Different orientations of carbon dioxide in the simulations represent the tumbling motion of the molecule before product formation. (*B* and *E*) Hydration sites located within 5 Å of the C_α obtained with SSTMap. (*C* and *F*) Minimum free-energy paths from the C2-ene adduct through the enolate to the products (2*S*)-ethylmalonyl-CoA and $NADP^+$. Parameter *D* represents the distance between C_α and C_2 minus the distance between C_α and CO_2.

binding, which explains the experimentally observed increased K_M for CO_2. In our simulations, the CO_2 molecule shows an increased rotational tumbling at the active site of the H365N variant compared with the WT, which is reflected by an increased rmsd for CO_2 (2.4 Å versus 0.46 Å). Together, experiment and simulations indicated reduced carboxylation efficiency because of decreased control of CO_2 (but not water) at the active site in the H365N variant, lowering the chances of productive Michaelis complex formation.

Similar to the H365N variant, replacement of Glu171 with alanine also resulted in a k_{cat} decrease (17-fold), and carboxylation of crotonyl-CoA was also maintained (97%). Additionally, however, the K_M for crotonyl-CoA increased 25-fold, indicating an additional role of Glu171 in positioning the CoA substrate. In our simulations of the E171A mutant, interaction of CO_2 with Asn81 is partially maintained, while Phe170 adopts the position of the mutated glutamate in the WT (Fig. 3*A* and Movie S5). As for H365N, the E171A variant showed increased CO_2 tumbling at the active site, which is reflected by an rmsd of 2.0 Å (compared with 0.46 Å of the WT). Altogether, these results suggest that in the E171A variant, similar to the H365N variant, control of the CO_2 molecule (but not water) is affected.

While H365N and E171A show a similar carboxylation behavior, the free-energy paths of the 2 variants show distinct differences (Fig. 3 *C* and *F*). In both variants, the 2 main barriers along the minimum free-energy path of the reaction—the one that leads to the enolate from the C2-ene adduct and the one that adds CO_2 to the enolate—appear increased compared with the WT (for WT see Fig. 2*C*). This is experimentally reflected by the decreased catalytic activity of the 2 variants and can be related to a distorted water network and increased tumbling of CO_2 at the active site of these enzymes. In H365N, however, the first energy barrier is higher compared with E171A. This indicates that enolate formation is disfavored and suggests that the C2-ene adduct accumulates in the H365N variant. This was experimentally confirmed by measuring the stereospecificity of the reduction reaction in the absence of CO_2. In the H365N variant, stereospecificity was lost (Table 1), indicating that the H365N is additionally affected in enolate formation compared with the E171A mutant and the WT, respectively.

In summary, His365 and Glu171 can partially compensate each other so that carboxylation function is maintained. However, only the combined action of the 2 residues allows full control over the CO_2 molecule and thus a fast carboxylation rate.

Discussion

Ccr from *K. setae* carboxylates crotonyl-CoA at a turnover frequency of more than 100 s^{-1}. This is almost 1 order of magnitude faster than an average RuBisCO homolog and one of the fastest CO_2-conversion rates described to date. Combining X-ray crystallography, experimental biochemistry, and molecular dynamics simulations we characterized the role of individual amino acids at the active site of KsCcr in CO_2 binding and C–C-bond formation. In KsCcr the active site is optimized to accommodate CO_2 and at the same time exclude water to suppress the competing reduction reaction. All this is apparently achieved by only 4 amino acids: Asn81, His365, Glu171, and Phe170. The amide group of Asn81 is responsible for anchoring the CO_2 from one side, while a water network organized from an ordered water molecule coordinated between His365 and Glu171 serves as an additional anchor point for CO_2 from the opposite side. The aromatic ring of Phe170 side chain actively prevents the diffusion of water into the active site.

Why is the CO_2-fixation reaction of Ecrs so much faster but still more specific compared with the reaction catalyzed by RuBisCO, although both enzymes react through an enolate? Note that there are fundamental differences in the catalytic mechanisms of RuBisCO and Ecrs. In RuBisCO, enolization of the substrate ribulose 1,5-bisphosphate is achieved by abstraction of the H3 proton through an active-site carbamylated lysine, which is a reversible process and very close to equilibrium (24). (Re)protonation of the enolate yields the substrate again, which can undergo another round of activation until it reacts with a CO_2 (or O_2) molecule, which pulls the reaction further (25). In contrast, in Ecrs the enolate is formed by hydride transfer from NADPH to the β-position of crotonyl-CoA (17–19). This provides a more "unidirectional" reaction path and leaves the enolate committed for a nucleophilic attack. Accordingly, Ecrs are required to carefully control the further fate of the enolate and especially to prevent its protonation, which would irreversibly quench the reaction (in stark contrast to the case of RuBisCO). When CO_2 is absent from the active site of WT Ecr (18), or its positioning is disturbed (e.g., by H365N or N81L mutation, this study), the enolate is not simply transformed back into the starting substrates as in RuBisCO, but tends to collapse into the C2-ene adduct, which is in line with the idea of unidirectionality in Ecr catalysis. It might be tempting to speculate that the C2-ene adduct serves as a way to "store" the reactive enolate until a resolving CO_2 electrophile becomes available, thereby increasing the overall reactivity of Ecrs compared with RuBisCOs.

RuBisCO and Ecrs probably both evolved from non–CO_2-fixing ancestors. While it has been speculated that RuBisCO emerged from an ancestral sugar phosphate isomerase it is thought that Ecrs evolved from a primordial enoyl-CoA reductase (6, 26). Clearly, this put more constraints onto the active-site topology of Ecrs, because unlike the CO_2 fixation reaction in RuBisCO that could be simply built on top of a reversible isomerization reaction, the reduction reaction needed to be suppressed and replaced by the carboxylation reaction in the Ecr scaffold because of the unidirectionality of Ecr's catalytic mechanism. The situation is reminiscent of 2-ketopropyl coenzyme M oxidoreductase/carboxylase that evolved within the superfamily of NAD(P)H disulfide oxidoreductases for which the enzyme also had to replace an active-site topology prone to reduction reactions by a CO_2-fixing active site (11). In both cases, the active-site transformation was achieved with only little changes and notably without introduction of a competing oxygenation reaction, posing the question whether the evolutionary circumstances or the nature of the catalytic cycle of both enzymes were responsible to achieve this superior selectivity against oxygen compared with RuBisCO.

In summary, our findings provide detailed insights into the molecular control of CO_2 at one of nature's most efficient carbon-fixing enzymes. These insights will be helpful in the future design of catalytic frameworks for the capture and conversion of CO_2 in chemistry and biology (27), but also for efforts that aim at using Ecrs as key enzymes in the development of synthetic cycles for the sustainable and efficient fixation of CO_2 (28, 29).

Materials and Methods

Chemicals. Crotonic Anhydride and Carbonic anhydrase from bovine erythrocytes were purchased from Sigma-Aldrich AG, CoA trilithium salt and DNase I from Roche Diagnostics, and NADPH Na_4 (98%) from Carl Roth GmbH. Solvents and salts were all analytical grade or better. Crotonyl-CoA was synthesized as previously reported (30).

Cloning and Mutagenesis. The KsCcr gene was provided by the Joint Genome Institute. Enzyme variants were generated with the QuikChange Site-Directed Mutagenesis Kit (Stratagene) using primer pairs listed in *SI Appendix*, Table S2.

Protein Expression and Purification. Details about expression and purification are described in *SI Appendix*.

Quantification of Reaction Products. Details about quantification of reaction products are described in *SI Appendix*.

Spectrophotometric Enzyme Assays. Assays were performed on a Cary-60 UV/Vis spectrophotometer (Agilent) at 30 °C using quartz cuvettes (1- or 10-mm path length; Hellma). Reactions contained 20 μg/mL carbonic anhydrase and were performed in 100 mM K_2HPO_4 pH = 8.0. Kinetic parameters for 1 substrate were determined by varying its concentration while the others were kept constant at 10× their K_M value. Reaction procedure was monitored by following the oxidation of NADPH at 365 nm ($\varepsilon_{NADPH,365nm}$ = 3.33 $mM^{-1}{\cdot}cm^{-1}$). Each concentration was measured in triplicates and the obtained curves were fit using GraphPad Prism 8. Hyperbolic curves were fit to the Michaelis–Menten equation to obtain apparent k_{cat} and K_M values. For mutants revealing substrate inhibition, the data were fit to $v_0 = (V_{Max}[S])/(K_M + [S]((1 + [S])/K_i))$.

Determining the Stereochemistry of Protonation. Isotopic label incorporation experiments were performed analogous to a previously described method (*SI Appendix*, Fig. S4) (22).

Molecular Dynamics Simulations. Description of the workflow of the molecular dynamics simulations is described in *SI Appendix*.

ACKNOWLEDGMENTS. D.A.S. and E.V.-M. acknowledge K. Zinovjev for the implementation of the adaptive string method and fruitful discussions. Diffraction data were collected at Advanced Photon Source Beamline 23ID-B, Argonne National Laboratory. This work was supported by the European Research Council Grant 637675 (Combining synthetic biology and chemistry to create novel CO_2-fixing enzymes, organelles and organisms; SYBORG) granted to T.J.E., and the Max-Planck-Society Partnergroup Program, granted to E.V.-M. D.A.S. was supported by a SYNMIKRO fellowship. H.D. acknowledges support from NSF Science and Technology Centers Grant NSF-1231306 (Biology with X-ray Lasers, BioXFEL). S.W. acknowledges support from U.S. Department of Energy (DOE) Office of Science, Biological and Environmental Research; Stanford Precourt Institute; and SLAC Laboratory Directed Research and Development. The work conducted by the DOE Joint Genome Institute, a DOE Office of Science User Facility, is supported under Contract DE-AC02-05CH11231.

1. T. J. Erb, Carboxylases in natural and synthetic microbial pathways. *Appl. Environ. Microbiol.* **77**, 8466–8477 (2011).
2. R. J. Ellis, Most abundant protein in the world. *Trends Biochem. Sci.* **4**, 241–244 (1979).
3. R. Phillips, R. Milo, A feeling for the numbers in biology. *Proc. Natl. Acad. Sci. U.S.A.* **106**, 21465–21471 (2009).
4. E. Alper, O. Y. Orhan, CO_2 utilization: Developments in conversion processes. *Petroleum* **3**, 109–126 (2017).
5. M. Aresta, A. Dibenedetto, Utilisation of CO_2 as a chemical feedstock: Opportunities and challenges. *Dalton Trans.*, 2975–2992 (2007).
6. L. Schada von Borzyskowski, R. G. Rosenthal, T. J. Erb, Evolutionary history and biotechnological future of carboxylases. *J. Biotechnol.* **168**, 243–251 (2013).
7. D. L. Edmondson, H. J. Kane, T. J. Andrews, Substrate isomerization inhibits ribulosebisphospate carboxylase-oxygenase during catalysis. *FEBS Lett.* **260**, 62–66 (1990).
8. G. Bowes, W. L. Ogren, R. H. Hageman, Phosphoglycolate production catalyzed by ribulose diphosphate carboxylase. *Biochem. Biophys. Res. Commun.* **45**, 716–722 (1971).
9. G. A. Prussia *et al.*, Substitution of a conserved catalytic dyad into 2-KPCC causes loss of carboxylation activity. *FEBS Lett.* **590**, 2991–2996 (2016).
10. M. A. Kofoed, D. A. Wampler, A. S. Pandey, J. W. Peters, S. A. Ensign, Roles of the redox-active disulfide and histidine residues forming a catalytic dyad in reactions catalyzed by 2-ketopropyl coenzyme M oxidoreductase/carboxylase. *J. Bacteriol.* **193**, 4904–4913 (2011).
11. A. S. Pandey, D. W. Mulder, S. A. Ensign, J. W. Peters, Structural basis for carbon dioxide binding by 2-ketopropyl coenzyme M oxidoreductase/carboxylase. *FEBS Lett.* **585**, 459–464 (2011).
12. B. Stec, Structural mechanism of RuBisCO activation by carbamylation of the active site lysine. *Proc. Natl. Acad. Sci. U.S.A.* **109**, 18785–18790 (2012).
13. M. van Lun, J. S. Hub, D. van der Spoel, I. Andersson, CO2 and O2 distribution in Rubisco suggests the small subunit functions as a CO2 reservoir. *J. Am. Chem. Soc.* **136**, 3165–3171 (2014).
14. Y. Ito, H. Kondo, Y. Shiota, K. Yoshizawa, Theoretical analysis of the reaction mechanism of biotin carboxylase. *J. Chem. Theory Comput.* **4**, 366–374 (2008).
15. D. M. Peter *et al.*, Screening and engineering the synthetic potential of carboxylating reductases from central metabolism and polyketide biosynthesis. *Angew. Chem. Int. Ed. Engl.* **54**, 13457–13461 (2015).
16. T. J. Erb *et al.*, Synthesis of C5-dicarboxylic acids from C2-units involving crotonyl-CoA carboxylase/reductase: The ethylmalonyl-CoA pathway. *Proc. Natl. Acad. Sci. U.S.A.* **104**, 10631–10636 (2007).
17. T. J. Erb, V. Brecht, G. Fuchs, M. Müller, B. E. Alber, Carboxylation mechanism and stereochemistry of crotonyl-CoA carboxylase/reductase, a carboxylating enoyl-thioester reductase. *Proc. Natl. Acad. Sci. U.S.A.* **106**, 8871–8876 (2009).
18. R. G. Rosenthal *et al.*, Direct evidence for a covalent ene adduct intermediate in NAD(P)H-dependent enzymes. *Nat. Chem. Biol.* **10**, 50–55 (2014).
19. R. G. Rosenthal *et al.*, The use of ene adducts to study and engineer enoyl-thioester reductases. *Nat. Chem. Biol.* **11**, 398–400 (2015).
20. N. Quade, L. Huo, S. Rachid, D. W. Heinz, R. Müller, Unusual carbon fixation gives rise to diverse polyketide extender units. *Nat. Chem. Biol.* **8**, 117–124 (2011).
21. L. Zhang *et al.*, Rational control of polyketide extender units by structure-based engineering of a crotonyl-CoA carboxylase/reductase in antimycin biosynthesis. *Angew. Chem. Int. Ed. Engl.* **54**, 13462–13465 (2015).
22. B. Vögeli *et al.*, InhA, the enoyl-thioester reductase from *Mycobacterium tuberculosis* forms a covalent adduct during catalysis. *J. Biol. Chem.* **293**, 17200–17207 (2018).
23. R. D. Libby, R. A. Mehl, Characterization of covalent Ene adduct intermediates in "hydride equivalent" transfers in a dihydropyridine model for NADH reduction reactions. *Bioorg. Chem.* **40**, 57–66 (2012).
24. G. Tcherkez, Modelling the reaction mechanism of ribulose-1,5-bisphosphate carboxylase/oxygenase and consequences for kinetic parameters. *Plant Cell Environ.* **36**, 1586–1596 (2013).
25. G. G. Tcherkez, G. D. Farquhar, T. J. Andrews, Despite slow catalysis and confused substrate specificity, all ribulose bisphosphate carboxylases may be nearly perfectly optimized. *Proc. Natl. Acad. Sci. U.S.A.* **103**, 7246–7251 (2006).
26. T. J. Erb, J. Zarzycki, A short history of RubisCO: The rise and fall (?) of Nature's predominant CO_2 fixing enzyme. *Curr. Opin. Biotechnol.* **49**, 100–107 (2018).
27. A. M. Appel *et al.*, Frontiers, opportunities, and challenges in biochemical and chemical catalysis of CO2 fixation. *Chem. Rev.* **113**, 6621–6658 (2013).
28. T. Schwander, L. Schada von Borzyskowski, S. Burgener, N. S. Cortina, T. J. Erb, A synthetic pathway for the fixation of carbon dioxide in vitro. *Science* **354**, 900–904 (2016).
29. A. Bar-Even, E. Noor, N. E. Lewis, R. Milo, Design and analysis of synthetic carbon fixation pathways. *Proc. Natl. Acad. Sci. U.S.A.* **107**, 8889–8894 (2010).
30. D. M. Peter, B. Vögeli, N. S. Cortina, T. J. Erb, A chemo-enzymatic road map to the synthesis of CoA esters. *Molecules* **21**, 517 (2016).